APPLICATIONS OF CHARGE TRANSFER DEVICES TO COMMUNICATION

D. D. Buss
Texas Instruments
Dallas, Texas

W. H. Bailey
Texas Instruments
Dallas, Texas

ABSTRACT

Charge transfer devices (CTD's) are analog in operation, and as such, they are uniquely applicable to many analog signal processing functions in the areas of communication, radar, sonar, guidance and control, etc. This paper is limited to military communication systems and addresses the following topics: (1) matched filtering in spread spectrum communication, (2) bandpass and low pass filtering, (3) Hilbert transform for single sideband modulation, (4) complex coding for M-ary communication, and (5) adaptive equalization for MODEM's.

The CTD transversal filter which is the fundamental building block for the above applications is described and the effect of imperfect charge transfer efficiency on its performance characteristics is determined. Examples of CTD filters are drawn from both charge coupled devices (CCD's) and bucket brigade devices (BBD's). However, design and fabrication techniques are not covered. This paper also summarizes CTD characteristics such as charge transfer efficiency, dynamic range, tap weight error, leakage and bandwidth as they apply to communication filtering applications. It shows that the cost and power consumption with CTD filtering can be significantly lower than with conventional digital filtering.

Spread spectrum systems which utilize CTD's are compared with systems which utilize surface wave devices and those which perform the matched filtering digitally. Comparisons are made with respect to performance, cost, power, weight, and size. The effects of charge transfer loss and tap weight error on receiver sensitivity are calculated, and the ultimate performance limitations of CTD systems are delineated. Data are presented on an incoherent receiver which performs matched filtering at baseband with chirp signals of time bandwidth product $T_dW = 100$. Measurements of bit error probability show a .5 dB sensitivity loss from minimum bit error probability predicted for noncoherent FSK.

Results are presented on a 101-stage CCD bandpass filter having Dolph-Chebyshev weighting and the characteristics of this filter are discussed. The remaining topics are covered briefly.

I. INTRODUCTION

Charge Transfer Devices (CTD's) are analog, sampled data delay lines, and as such they are readily applicable to a large number of analog signal processing functions. Certain types of sampled data filters which have, up until now, been implemented digitally,[1] can be realized in integrated form with CTD's. This paper discusses the advantages and limitations of CTD's for sampled data filtering in military communication systems.

CTD's include two important classes of device which are functionally very similar: charge coupled devices[2] (CCD's), and bucket brigade devices[3] (BBD's). CCD's are by far the better known, and although they were first announced a scant three years ago,[4] they are already commercially available. BBD's are older than CCD's and can be fabri-

cated using conventional MOS processes. CCD's require non-standard processing, but they have performance advantages over BBD's and will probably dominate analog signal processing in the future.

The basic building block which is used in the applications covered in this paper is the transversal, non-recursive CTD filter. Techniques for designing and making CTD transversal filters are described in the literature[5,6,7] and are not discussed here. Instead, this paper deals with those properties of CTD filters that determine their performance in communication filtering applications.

Since the impulse response of a CTD filter can be chosen arbitrarily, CTD filters can be matched to arbitrary signaling waveforms in much the same way that surface wave devices (SWD's) are used to perform matched filtering.[8] CTD's do not compete directly with SWD's for this application, however, because SWD's have higher bandwidth and limited time delay. CTD's on the other hand are capable of processing signals of up to 1 sec in time duration but are more restricted in bandwidth.

The competition faced by CTD's for this application is conventional digital processing, and that comparison can be summarized as follows. Compared with digital implementations, CTD filters are less flexible and are limited to time bandwidth (T_dW) products of 10^3 or less. On the other hand, when CTD's can be used for a particular matched filtering function, overwhelming advantages in cost, power consumption, size, weight, and reliability can be realized.

Section II of this paper gives a mathematical treatment of CTD transversal filters. Dispersion which results from imperfect charge transfer is characterized, and its effect on matched filter sensitivity is calculated. An example of a CCD matched filter is given.

Section III discusses the system aspects of CTD spread-spectrum receivers, and test results on a breadboard system are given.

Section IV discusses bandpass and lowpass filtering, Hilbert transform for single side band modulation, complex coding for M-ary communication, and adaptive equalization for MODEM's.

Section V concludes the paper with a discussion of the future of CTD's in military spread-spectrum systems.

II. CTD TRANSVERSAL FILTERS

A block diagram of a CTD, sampled data, transversal filter is given in Fig. 1. It consists of M delay stages D_k, k = 1, M, together with circuitry for performing the weighted summation of the node voltages v_k. Each delay stage consists of p transfer electrodes in a p-phase CTD (e.g. p = 3 for a 3-phase device). The input to the filter is sampled at the clock frequency f_c, and the delay of each stage is $T_c \equiv 1/f_c$. The filter output is given by

$$v_{out}(nT_c) = \sum_{k=1}^{M} h_k \, v_k(nT_c) \qquad (1)$$

$$= \sum_{k=1}^{M} h_k \, v_{in}[(n-k)T_c] \qquad (2)$$

$$v_{out}(t) \approx \int_0^{T_d} h(\tau) \, v_{in}(t-\tau) \, d\tau \qquad (3)$$

where $T_d = MT_c$ is the total time delay of the filter, and h(t) is the impulse response which has samples $h_k = h(kT_c)$.

A. DISPERSION DUE TO CHARGE TRANSFER LOSS

The filter described above has ideal delay stages, but CTD delay lines are not ideal. The CTD operates by transferring charge from one storage location to the next, and each time a transfer is made, a fraction α of the charge is lost. This fractional loss per transfer α is related to the fractional loss per delay stage ϵ by the number of transfers p required to accomplish one stage of delay.

$$\epsilon = p\alpha \qquad (4)$$

For CCD's p = 2, 3, or 4 and typically $\alpha \approx 10^{-4}$. For BBD's p = 2 and $\alpha \approx 10^{-3}$ although $\alpha \approx 10^{-4}$ can be achieved using the tetrode configuration.[9]

The effect of charge transfer loss can most easily be described by defining the z-transform of the k^{th} node voltage $V_k(z)$. Using this, imperfect charge transfer can be characterized by the relation

$$V_{k+1}(z) = z^{-1} \left[\epsilon V_{k+1}(z) + (1-\epsilon) V_k(z)\right] \qquad (5)$$

which can be solved to give

$$V_{k+1}(z) = \left(\frac{1-\epsilon}{1-\epsilon z^{-1}}\right) z^{-1} V_k(z) \qquad (6)$$

Eq. 6 is the fundamental transfer relation and reduces to the ideal delay relation when $\epsilon = 0$.

The relation between $V_1(z)$ and $V_{in}(z)$ depends upon the actual input circuit.[10] However, the differences which result are insignificant. For simplicity we will choose the input technique which results in

$$V_1(z) = \left(\frac{1-\epsilon}{1-\epsilon z^{-1}}\right) z^{-1} V_{in}(z) \qquad (7)$$

Combining eqs. 1, 6, and 7 gives

$$V_{out}(z) = \sum_{k=1}^{M} \left(\frac{1-\epsilon}{1-\epsilon z^{-1}}\right)^k h_k z^{-k} V_{in}(z) \qquad (8)$$

from which the transfer function

$$H^{\epsilon}(z) = \sum_{k=1}^{M} \left(\frac{1-\epsilon}{1-\epsilon z^{-1}}\right)^k h_k z^{-k} \qquad (9)$$

can be defined. The superscript indicates that the transfer function depends upon ϵ. Note that if the ideal transfer function $H^I(z)$ is determined from eq. 9 by setting $\epsilon = 0$,

$$H^I(z) = \sum_{k=1}^{M} h_k z^{-k}, \qquad (10)$$

then the transfer function of eq. 9 can be obtained by replacing z in the ideal transfer function by

$$z' = \left(\frac{1-\epsilon z^{-1}}{1-\epsilon}\right) z \qquad (11)$$

Because in all cases of practical interest $\epsilon \ll 1$, eq. 11 can be well approximated by taking

$$z' \approx z\, e^{\epsilon(1-z^{-1})} \qquad (12)$$

The above discussion indicates that the dispersion due to charge transfer loss can be calculated by replacing z in the ideal transfer function with z'. That is

$$H^{\epsilon}(z) \approx H^I(z') \qquad (13)$$

The dispersion due to charge transfer loss can be viewed in the frequency domain by using the definition of z

$$z^{-1} = \exp[-i2\pi f/fc] \qquad (14)$$

together with eq. 13. The result is

$$H^{\epsilon}(f) \approx H^I(f') \qquad (15)$$

where

$$f' = f + \frac{\epsilon f_c}{2\pi}\left\{\sin(2\pi f/f_c) - i[1-\cos(2\pi f/f_c)]\right\}$$

(eq. 16). Eq. 16 states that charge transfer loss introduces a frequency shift which is both real and imaginary. At low frequency the real part dominates as can be seen by expanding eq. 16 in a Taylor series in f/f_c. For $f \ll f_c$

$$f' \approx f(1+\epsilon) \qquad (17)$$

B. DISPERSION COMPENSATION

If the dispersion due to charge transfer inefficiency is known, the filter can be designed to invert this dispersion. Consider a filter having an infinite number of sampling stages and weighting coefficients $h'_k, k=1,\infty$. Its transfer function $H^{\epsilon}(k)$ can be shown by expanding eq. 9 to be

$$H^{\epsilon}(z) = \sum_{k=1}^{\infty} \left[\sum_{j=0}^{k-1} h'_{k-j} \binom{k-1}{j} \epsilon^j (1-\epsilon)^{k-j}\right] z^{-k}$$

(eq. 18). By equating the terms in the rectangular brackets to the desired weighting coefficients h_k, the desired transfer function can be obtained, and the h'_k which give rise to the desired transfer function are obtained by iterating the relation

$$h'_k = \frac{\left[h_k - \sum_{j=1}^{k-1} h'_{k-j} \binom{k-1}{j} \epsilon^j (1-\epsilon)^{k-j}\right]}{(1-\epsilon)^k} \qquad (19)$$

Even if the desired impulse response is finite in time ($h_k = 0$ for $k > M$), the exact solution of eq. 19 requires an infinite number of coefficients h'_k. However, in most cases, the error which results in truncating the h'_k series at M terms is negligible.

This technique for compensating charge transfer loss has been demonstrated.[7] However, the technique is limited by the fact that ϵ

cannot always be predicted with sufficient accuracy, and that it varies with clock frequency and other operating parameters.

C. SENSITIVITY VS. CHARGE TRANSFER LOSS

A CTD transversal filter can be used to detect signals in the presence of noise, and for this application, the filter impulse response is chosen to be the time inverse of the signaling waveform. Such a filter is said to be matched to the signal, and the matched filtering theorem of statistical communication states that when the noise environment is white and additive the matched filter provides the optimum output signal-to-noise ratio (SNR).[11]

Charge transfer loss, however, introduces a slight mismatch between the filter and the signaling waveform and results in loss of sensitivity. It will now be shown how charge transfer loss affects the sensitivity of a CTD matched filter assuming no measures are taken to compensate for loss.

Consider a filter whose weighting coefficients are chosen to represent an impulse response h(t) which is matched to a particular signal waveform $v_s(t)$.

$$h(t) = (1/A)v_s(T_d - t); \qquad 0 < t < T_d \tag{20}$$

where A is the amplitude of the signal waveform and h(t) is normalized so that its maximum amplitude is unity.

When v_s is applied to an ideal filter (ϵ=0), the output is given by eq. 2

$$v_{out}(nT_c) = A \sum_{k=1}^{M} h_k \, h_{M-n+k} \tag{21}$$

and the correlation peak occurring at $t_M \equiv MT_c$ is

$$v_{out}(t_M) = A \sum_{k=1}^{M} h_k^2 \tag{22}$$

However, charge transfer loss changes the effective weighting coefficients of the filter to new values h_k^ϵ which can be calculated as in eq. 18 to be

$$h_k^\epsilon = \sum_{j=0}^{k-1} h_{k-j} \binom{k-1}{j} \epsilon^j \, (1 - \epsilon)^{k-j} \tag{23}$$

and the output signal at the correlation peak is

$$v_{out}(t_M) = A \sum_{k=1}^{M} h_k \, h_k^\epsilon \tag{24}$$

which can be written as

$$v_{out}(t_M) = \frac{A}{2\pi i} \oint H(z) \, H^\epsilon(z^{-1}) z^{-1} \, dz \tag{25}$$

$$\approx A \int_{-f_c/2}^{+f_c/2} H(f) \, H^*(f') \, df \tag{26}$$

In the above equations, H(z) and $H^\epsilon(z)$ are the z-transforms of h_k and h_k^ϵ respectively and f′ is given by eq. 16.

The peak output power

$$S_p = v_{out}^2(t_M) \tag{27}$$

can be calaulated from eq. 26 and decreases with increasing ϵ because charge transfer loss introduces an effective mismatch between the filter and the signal waveform.

However, charge transfer loss also affects the output noise power. If the input noise is assumed to be white and to have single sided spectral density N_o, the rms noise power is given by

$$N_p = \frac{N_o}{2} \frac{1}{2\pi i} \oint H^\epsilon(z) \, H^\epsilon(z^{-1}) \, z^{-1} \, dz \tag{28}$$

$$= \frac{N_o}{2} \int_{-f_c/2}^{+f_c/2} |H(f')|^2 \, df \tag{29}$$

provided the CTD matched filter is preceeded by an anti-aliasing filter which eliminates components of noise higher in frequency than $f_c/2$.

Under these conditions the output SNR ρ_{out} can be evaluated by combining eqs. 26, 27, and 29.

$$\rho_{out} \equiv \frac{S_p}{N_p}$$

$$= \frac{2A^2}{N_o} \frac{\left[\int_{-f_c/2}^{+f_c/2} H(f)\, H^*(f')\, df\right]^2}{\int_{-f_c/2}^{+f_c/2} |H(f')|^2\, df} \qquad (30)$$

Contact can be made with the familiar equation for the output SNR of a matched filter[11] by letting $\epsilon \to 0$. In this case

$$\rho_{out} \to \frac{2E_s}{N_o} \qquad (31)$$

where the signal energy E_s is given by

$$E_s = A^2 \int_{-f_c/2}^{+f_c/2} |H(f)|^2\, df \qquad (32)$$

A very useful result can be obtained by expanding eq. 30 in a Taylor series in ϵ. If ρ_{out} is written as

$$\rho_{out} = \frac{2E_s}{N_o} - \alpha\epsilon - \beta\epsilon^2 - \cdots \qquad (33)$$

then it can be shown that $\alpha = 0$. Even though the output signal power S_p decreases linearly with ϵ due to signal mismatch, the output noise power N_p also decreases proportionally, so that only terms second order and higher in ϵ contribute to sensitivity loss. This is extremely fortuitous because it allows one to design filters having fairly large dispersion (large $M\epsilon$ product) without seriously degrading sensitivity.

The above analysis is illustrated with calculations made on a 100-bit pn filter whose pseudorandom code is given in Table 1. The output peak signal power S_p and the output rms noise power N_p are normalized to their respective input values (A^2 and $N_o f_c/2$) and plotted in Fig. 2. Both quantities decrease linearly with ϵ but the output SNR ρ_{out} decreases much more slowly.

Fig. 2 can be used to determine an upper limit on the dispersion which can be tolerated in a matched filter. If it is arbitrarily specified that charge transfer loss degrade the sensitivity by no more than 90% (.5 dB), this requires the $M\epsilon$ product to be less than $\Gamma = .6$.

The Nyquist sampling theorem ($W < f_c/2$) together with the above limitation on $M\epsilon$ product ($M\epsilon < \Gamma$) leads to the following limitation on time bandwidth product T_dW:

$$T_dW \le M/2 \le \frac{\Gamma}{2\epsilon} \qquad (34)$$

Using $\epsilon = 3 \times 10^{-4}$ this gives $T_dW \le 10^3$.

D. OTHER LIMITATIONS

In addition to the loss which results when charge transfers from one storage location to another, CTD's lose charge due to leakage. This limits the total time delay which can be achieved to 1 sec. or less.

For all CTD's charge transfer loss increases severely at high frequencies, and although CCD's may eventually operate at hundreds of MHz, current technology limits CTD filters to 10 MHz or less.

These limitations, together with the T_dW limitation of the previous section, are illustrated in Fig. 3.

Tap weight error is the limiting factor in some CTD filtering applications.[12] However, for matched filtering applications, the additional "noise" introduced by random tap weight is negligible.[7]

E. EXAMPLE

The operation of a CCD filter is shown in Fig. 4. This device was designed using the electrode weighting technique[7] and the h_k coefficients are given in Table 1. No interelectrode gaps are present in the photomicrograph at the top of the figure because $|h_k| = 1$. The filter impulse response is shown at the center of the figure and the correlation response is shown at the bottom. Note the correlation peak in the output. The device shown had $M\epsilon \approx 0.1$, so the output waveform is essentially ideal.

III. SPREAD SPECTRUM COMMUNICATION USING CTD'S

As indicated in the previous section, CTD's are limited in frequency to around 10 MHz. Therefore, filtering in a CTD system must be performed at baseband in distinction to SWD systems where the filtering is performed at RF.

Figures 5 and 6 illustrate the difference between RF and baseband processing. Assume the signaling waveform is of the form

$$v_i(t) = A\, h_i(t) \cos(\omega_o t + \phi) \qquad i = 0, 1 \tag{35}$$

where ϕ is the unknown phase and where h_o and h_1 represent the two binary waveforms being transmitted. Figure 5 shows the RF processor in which the incoming signal is first filtered in a filter matched to the RF waveform and then envelope detected. Envelope detection is indicated here as a mixing operation followed by squaring and adding operations. In the baseband system of Fig. 6, the mixing and filtering operations are interchanged. The incoming RF signal is first mixed to baseband, and then filtered in a filter matched to the baseband signal. Both systems can be shown to have identical performance, and their bit error probability is equivalent to noncoherent FSK[13].

Equation 35 is not the most general type of narrow band signaling waveform which can be employed. The most general form is

$$v_i(t) = A\,[h_i(t) \cos(\omega_o t + \phi) + g_i(t) \sin(\omega_o t + \phi)] \qquad i = 0, 1 \tag{36}$$

This generalized waveform complicates the baseband processor of Fig. 6. Four filters are required matched to h_o, h_1, g_o, and g_1.

The discussion will now be specialized to chirp (linear FM) signaling systems. Chirp is particularly attractive because it is minimally sensitive to error in the local oscillator frequency, and this is expected to be a major problem in CTD spread spectrum systems.

The RF chirp signal can be written as:

$$v_i(t) = A \cos(\omega_o t \pm \mu t^2 + \phi) \qquad -T_d/2 < t < +T_d/2 \tag{37}$$

where i = 1 corresponds to an up-chirp (+) and i = 0 corresponds to a down-chirp (-). For convenience the time interval is taken to be symmetric about t = 0. The RF signal chirps through a bandwidth

$$W = \frac{\mu T_d}{\pi} \tag{38}$$

centered about $f_o = \frac{\omega_o}{2\pi}$.

The chirp signal of eq. 37 is of the form of eq. 36 as can be seen by expanding eq. 37. In this case

$$h_o = h_1 = \cos \mu t^2$$
$$g_o = -g_1 = \sin \mu t^2 \qquad -\frac{T_d}{2} < t < \frac{T_d}{2} \tag{39}$$

The use of chirp also simplifies receiver design somewhat because now two pairs of filters are required matched to the two signals of eq. 39.

A baseband system which can be used to detect binary chirp is shown in Fig. 7. The filters marked SIN and COS are matched to the signals of eq. 39. In a baseband system such as that of Fig. 7, the baseband signals chirp from -W/2 through zero to +W/2 or vice versa, and each filter has a bandwidth of only W/2. Therefore to recover all the information in the signal two filters are required, and their outputs must be added coherently as shown. The chirp through zero scheme has the further advantage of halving the bandwidth requirement on each filter. The 1 - 0 decision is made by comparing the up-chirp output with the down-chirp output at the time of the correlation peak.

The system of Fig. 7 was implemented using 200-stage BBD filters. The signaling waveforms have $T_dW = 100$ for an overall processing gain of 23 dB. To eliminate aliasing, the filters were designed to sample the impulse responses of eq. 39 at 2W, i.e. twice the Nyquist rate for the highest frequency. The responses of these filters to a negative impulse are shown in Fig. 8. The decrease in the amplitude of the impulse responses results from charge transfer loss which for these devices was $\alpha = 10^{-3}$. The sensitivity loss which this causes is calculated to be less than .1 dB. The correlation responses which result from a coherent chirp signal are also shown in Fig. 8. Fig. 9 shows the outputs of the up-chirp and down-chirp channels when the input signal is noncoherent, and chirps alternately up and down. Even when the input signal is

masked by noise the correlation peaks in the output are unambiguous.

The bit error probability P_e for a noncoherent FSK receiver is given by[13]

$$P_e = 1/2 \exp(-\gamma/2) \quad (40)$$

where

$$\gamma = \frac{E_s}{N_o} \quad (41)$$

E_s is the signal energy, and N_o is the single sided spectral density of the noise. The measured bit error probability is compared in Fig. 10 with eq. 40 and shows that the detector sensitivity is within .5 dB of the theoretical limit.

The measured dynamic range of the filters themselves is in excess of 75 dB, and they have been tested from -60°C to +80°C. Device performance improves at low temperature, but at higher temperature leakage current in both CCD's and BBD's limits low frequency (long T_d) operation.

IV. OTHER COMMUNICATION APPLICATIONS

Within the constraints of (27) - (29), the applicability of CTD's to sampled data filtering problems is limited only by the designer's imagination. Some of the more commonly occurring applications are discussed in this section.

A. BANDPASS FILTERING

A CTD transversal filter can be used to implement a bandpass filter by selecting the impulse response of the filter to be the inverse transform of the frequency characteristic.[12] The measured frequency response of such a filter implemented with CCD's is given in Fig. 11. This filter was designed using Dolph-Chebyshev weighting to achieve 29 dB rejection and a 3 dB bandwidth of 4% of the center frequency. The center of the passband occurs at $f_c/4$ and the filter is tunable by varying f_c.

Using this approach, it is difficult to achieve filters of high Q because of the finite time duration of the impulse response of a transversal filter, and because tap weight error limits the out-of-band rejection. Recursive filters are potentially useful for achieving high Q as has been demonstrated using BBD's[14] with off-chip feedback. However, until techniques are developed for integrating the required feedback, CTD recursive filters will not be generally applicable.

CTD transversal filters are most useful when the magnitude and phase of the frequency response must be accurately determined. They can also be used when the signal level is low (down to 50 μvolt) and have large dynamic range.

B. HILBERT TRANSFORM

A Hilbert Transform consists of a convolution with t^{-1} and can be implemented with a CTD transversal filter having weighting coefficients

$$h_k = \frac{1}{k - \frac{(M+1)}{2}} \qquad \begin{matrix} k = 1, M \\ M \text{ even} \end{matrix} \quad (42)$$

Such a filter can be used to generate single sideband signals [10] and has a wide potential application in communication equipment.

C. COMPLEX CODING

CTD filters can be used to generate as well as to detect arbitrary waveforms. This presents the possibility of choosing M waveforms to represent $k = \log_2 M$ bits of information. This type of coding is currently employed in MODEM's, but the choice of waveform is limited by the available equipment, and the waveforms actually used are not orthogonal or optimized to the transmission medium. CTD's offer a great deal of flexibility in selection of waveform. In addition, the relative ease with which CTD filters can be matched to arbitrary waveforms may make feasible the use of M-ary (instead of binary) communication where it has not previously been practical.

D. ADAPTIVE FILTERING

Due to the changing characteristics of a telephone channel, adaptive equalization is required in a MODEM. This requires a variable tap weight convolution filter (VTWCF), and although all CTD convolution filters reported to date have fixed weighting coefficients, a CTD VTWCF is feasible. Such a filter would be extremely useful not only in MODEM's but in other adaptive filtering applications such as voice recognition, adaptive beam forming, remote intrusion detec-

tion, etc.

V. CONCLUSIONS

The largest impact which CTD's will make on military communication systems is cost reduction of systems which are produced in sufficiently high volume to offset the development cost of a custom CTD filter. The cost comparison between CTD and digital implementations is extremely difficult because it must be made for each system. However, for illustrative purposes we will give a simple example.

It is required to implement a 100 point convolution filter with a dynamic range which requires 8-bit digital logic. An analog signal is to be sampled at 100 kHz, filtered and presented at the output in analog form. When this filtering operation is implemented using TTL the cost and power consumption are determined primarily by the 8-bit A/D converter ($2000, 5W) and the digital filter (approximately 400 TTL networks costing $5 apiece and dissipating 100 mW apiece).

In evaluating the cost of the CTD implementation the important factor of part volume enters. The digital filter can be implemented with standard catalog items whereas the CTD is a custom IC, and as such its cost is strongly dependent upon the number of parts required. A reasonable approach to calculating the price of a CTD custom chip is to assume 80 k$ development cost plus $5 per copy. Using this, the price per copy p_c would be

$$p_c = \$5 + \frac{\$8 \times 10^4}{N_u} \qquad (43)$$

where N_u is the total number of units required. If $N_u = 80{,}000$ then $p_c = \$6$ for the CTD. In addition to the CTD, circuitry is required for clock drivers, output amplifiers and output sample-and-hold. The total cost for these parts is less than $50, and the power dissipation is on the order of 600 mW.

A summary of this comparison is given below:

	Digital	CTD
Cost	$4000	$56
Power	45W	600mW

This comparison is an oversimplification of real systems, and it is heavily weighted in favor of CTD's because it is based upon a simple convolution filtering operation for which CTD's are ideally suited. However, it illustrates the saving in cost and power which is possible with CTD's.

CTD's have potential advantages in small size and low weight which result from the compactness of the filter IC and potential advantages in increased reliability which result from a reduction in the number of package interconnects required.

Communication is an important field which appears to be ideally suited to capitalize on the advantages of CTD filtering. Progress has been made in developing CTD technology for these applications, and continued development at this time is amply justified.

ACKNOWLEDGEMENTS

Most of the work presented in this paper was sponsored by Rome Air Development Center under contract #F30602-73-C-0027 and directed by Charles N. Meyer of RADC. Development of the CCD filter of Fig. 4 was sponsored by the Naval Electronics Command under contract #N00039-73-C-0013 and directed by Dr. David F. Barbe of N.R.L. Development of the CCD bandpass filter discussed in Sec. IV-A was sponsored by the U. S. Army Electronics Command under contract #DAAB07-73-C-0266, and directed by Ted J. Lukaszek of Ft. Monmouth.

REFERENCES

1. B. Gold and C. M. Rader, Digital Processing of Signals, McGraw-Hill, 1966.
2. W. S. Boyle and G. E. Smith, "Charge Coupled Semiconductor Devices," Bell Syst. Tech. J., 49, pp. 587-593, April 1970.
3. F. L. J. Sangster, "Integrated MOS and Bipolar Analog Delay Lines Using Bucket-Brigade Capacitor Storage," in 1970 IEEE Solid-State Circuits Conf., Dig. Tech. Papers, pp. 74-75, 185.
4. Fairchild's CCD 101 is a 500-element CCD linear image sensor.
5. D. D. Buss, W. H. Bailey and D. R. Collins, "Matched Filtering Using Tapped Bucket-Brigade Delay Lines," Elec. Lett. 8, pp. 106-107, 4 Jan. 1972.

6. D. R. Collins, W. H. Bailey, W. M. Gosney and D. D. Buss, "Charge-Coupled Device Analog Matched Filters," Elec. Lett. 8 pp. 328-329, June 29, 1972.
7. D. D. Buss, D. R. Collins, W. H. Bailey and C. R. Reeves, "Transversal Filtering Using Charge Trasnfer Devices," IEEE J. Solid-State Circuits, SC-8, pp. 138-146, April 1973.
8. D. T. Bell, Jr., J. D. Holmes, and R. V. Ridings, "Applications of Acoustic Surface Wave Technology to Spread Spectrum Communications" (Invited Paper) IEEE Tran. Microwave Theory Tech., MTT-21, pp. 263-271, April 1973.
9. L. Boonstra and F. L. J. Stangster, "Progress on Bucket-Brigade Charge-Transfer Devices" in 1972 IEEE Solid-State Circuits Conf., Dig. Tech. Papers, pp. 140-141, 228.
10. D. D. Buss, W. H. Bailey and D. R. Collins, "Analysis and Applications of Analog CCD Circuits," Proceedings of 1973 International Symposium on Circuit Theory, April 9-11, 1973, Toronto, pp. 3 - 7.
11. M. Schwartz, W. R. Bennett and S. Stein, Communication Systems and Techniques, McGraw-Hill, 1966, pp. 63 - 68.
12. D. D. Buss, D. R. Reeves, W. H. Bailey and D. R. Collins, "Charge Transfer Devices in Frequency Filtering," Proceedings of the 26th Annual Symposium on Frequency Control, June 6 - 8, 1972, Atlantic City, N.J., pp. 171-179.
13. M. Schwartz, W. R. Bennett and S. Stein, Op. Cit., pp. 81-82, 297-299.
14. D. A. Smith, C. M. Puckette, and W. J. Butler, "Active Bandpass Filtering with Bucket-Brigade Delay Lines," IEEE J. Solid-State Circuits, SC-7, pp. 421-425, October 1972.

FIGURES

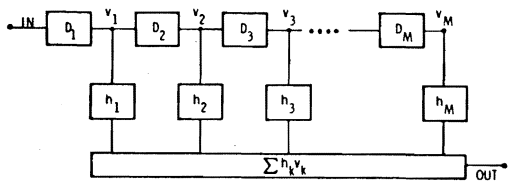

Fig. 1 Block diagram of a transversal filter consisting of M delay stages D_k and M weighting coefficients h_k.

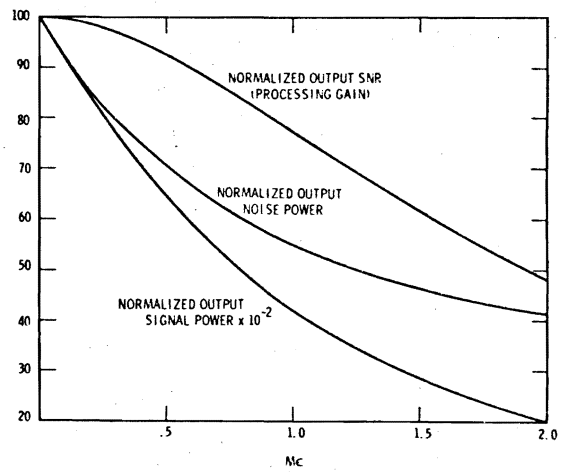

Fig. 2 Signal power, noise power, and SNR at the output of the 100-bit filter described in the text. These results are normalized to their respective quantities at the input to the filter and plotted as a function of the loss parameter Mε.

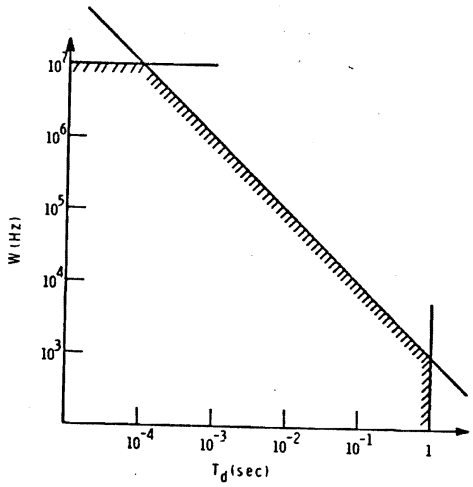

Fig. 3 The approximate limitations on the time duration (T_d) and bandwidth (W) of signals which can be processed using CTD's. $T_d \leq 1$ sec, $W \leq 10$ MHz, $T_d W \leq 10^3$.

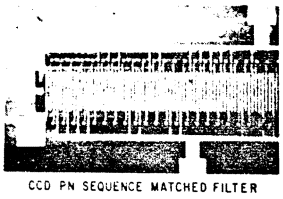

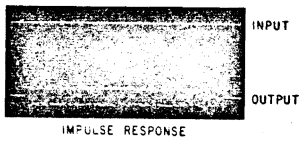

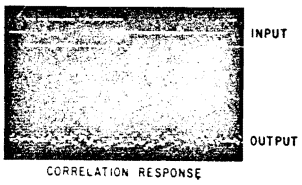

Fig. 4 (above) Operation of a 100-bit pn sequence CCD filter matched to a pseudorandom code. Top: Photomicrograph of the first few stages of the filter. Center: Response of the filter to a negative impulse. Bottom: Correlation response of the filter. Note the correlation peak in the output waveform.

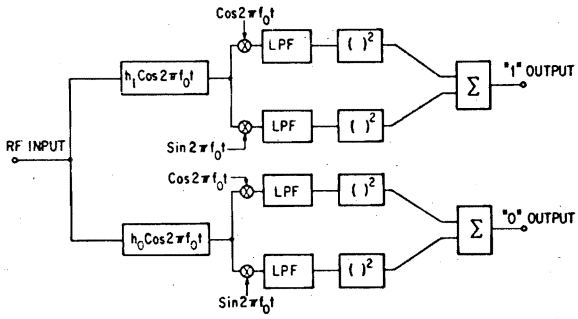

Fig. 5 Block diagram of a binary RF processor.

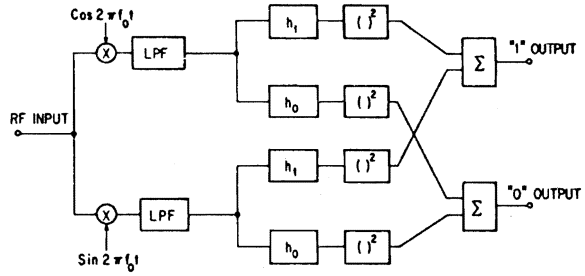

Fig. 6 Block diagram of a binary baseband processor.

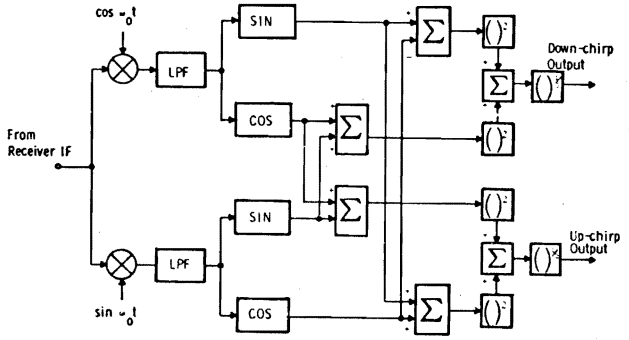

Fig. 7 A receiver for binary chirp waveforms. The boxes labeled COS and SIN are BBD filters whose characteristics are shown in Fig. 8.

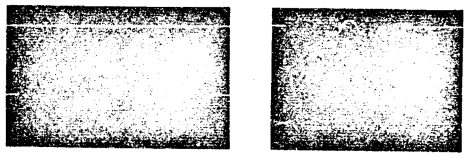

$h(t) = \cos \omega t^2$

$-\frac{T_d}{2} < t < \frac{T_d}{2}$

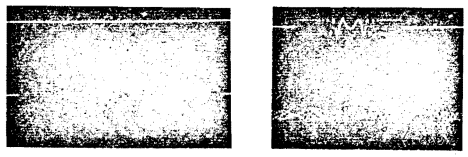

$g(t) = \sin \omega t^2$

$-\frac{T_d}{2} < t < \frac{T_d}{2}$

Fig. 8 The impulse response and correlation response of the two filters required for the system of Fig. 7. These filters are each 200 stages long and are both integrated in a single BBD IC.

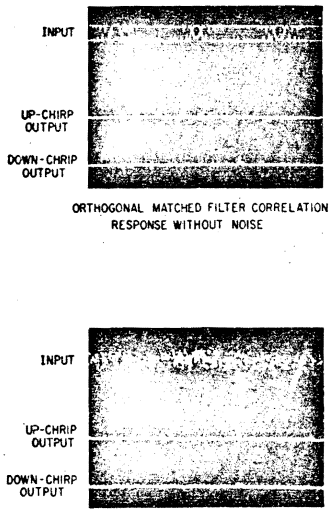

Figure 9. The outputs of the receiver of Fig. 7 when noncoherent up-chirp and down-chirp signals are sequentially applied to the input. Even when the input is obscured by noise, the output is unambiguous.

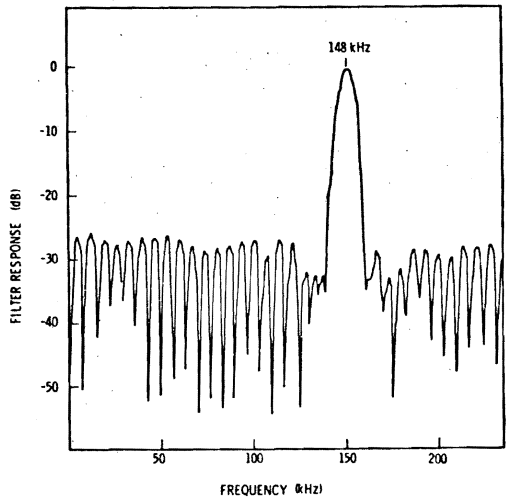

Fig. 11 The measured frequency response of a 101-stage Dolph-Chebyshev CCD bandpass filter. The filter was designed to have 29 dB out-of-band rejection and tunable passband at .25 f_c

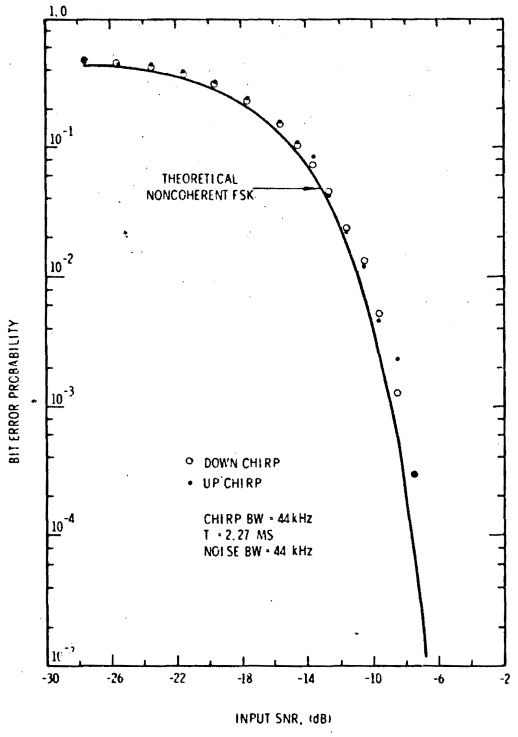

Fig. 10 Measured bit error probability P_e of the receiver of Fig. 7. The overall sensitivity was found to be .5 dB less than the ideal sensitivity for noncoherent FSK.

TABLE I

Code for the 100-Bit pn Sequence Filter

The time signal consists of the elements of this table in the order given. The filter itself is coded with these values in reverse order.

1 - 10	-	+	+	-	-	+	-	+	+	-
11 - 20	-	-	-	+	+	-	-	+	-	-
21 - 30	+	-	-	-	+	+	-	+	+	+
31 - 40	+	+	+	+	-	+	-	-	+	+
41 - 50	-	+	+	-	+	-	-	+	-	-
51 - 60	-	-	-	-	-	+	+	-	-	-
61 - 70	+	+	+	-	+	-	-	-	+	-
71 - 80	+	+	+	+	+	-	+	+	-	-
81 - 90	+	-	+	+	+	+	+	-	-	+
91 - 100	+	-	-	+	+	+	-	-	-	-

REVERSE SIDE BLANK